Support Information

Figure Captions

Fig. S1. XPS spectra of Sn on Sn-graphite.

Fig. S2. Recovery and reuse of Sn-graphite for catalyzing BSS.

Fig. S3. Effects of cosubstrate glucose loading on FF-reducing activity of CCZU-A13 cells.

Fig. S4. Effects of various temperature on FF-reducing on activity of CCZU-A13 cells (a); Effects of various pH on FF-reducing catalytic activity of CCZU-A13 cells (b).

Fig. S5. Effects of amine donor IPA loading on the bioamination activity of AT2018 cells.

Fig. S6. Effects of various temperature on FF-amination activity of AT2018 cells (a); Effects of various pH on FF-amination activity of AT2018 cells (b).

Table Caption

Table S1. Changes of Sn content on Sn-graphite by element analysis before and after repeated use of Sn-graphite

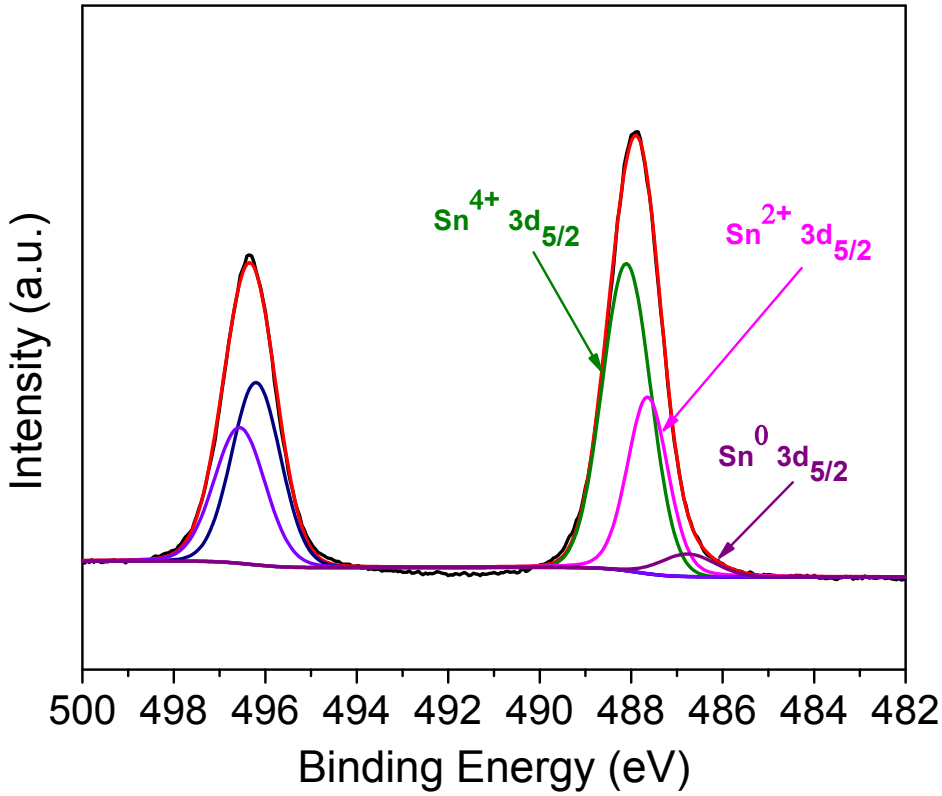

Name	Peak BE	FWHM (eV)	Area (P) CPS.eV	Fraction (%)
Sn^{0} $3d_{5/2}$	486.76	1.40	3052.253	5.2
Sn^{2+} $3d_{5/2}$	487.64	1.04	19108.1	32.3
Sn^{4+} $3d_{5/2}$	488.1	1.24	36967.78	63.5

Fig. S1. XPS spectra of Sn on Sn-graphite

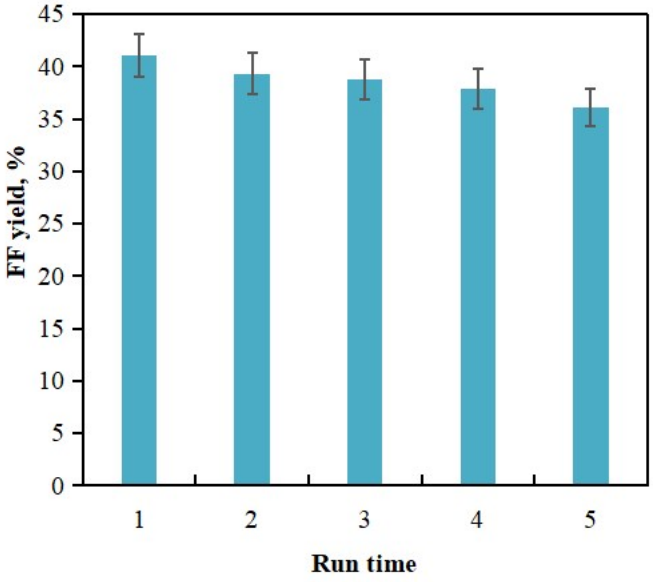

Fig. S2. Recovery and reuse of Sn-graphite for catalyzing BSS.

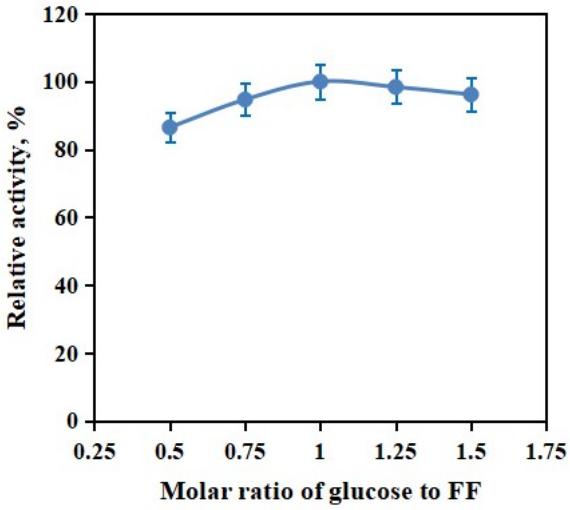

Fig. S3. Effects of cosubstrate glucose loading on FF-reducing activity of CCZU-A13 cells.

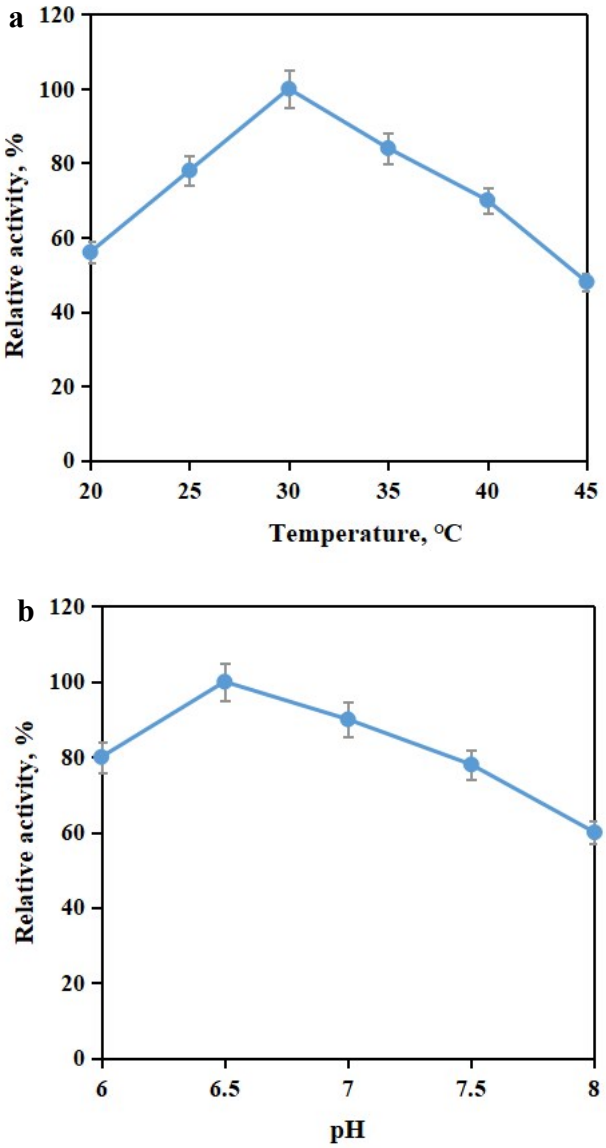

Fig. S4. Effects of various temperature on FF-reducing on activity of CCZU-A13 cells (a); Effects of various pH on FF-reducing catalytic activity of CCZU-A13 cells (b).

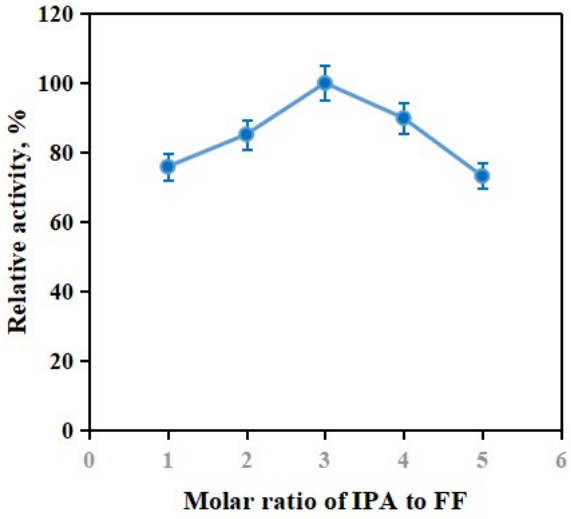

Fig. S5. Effects of amine donor IPA loading on the bioamination activity of AT2018 cells.

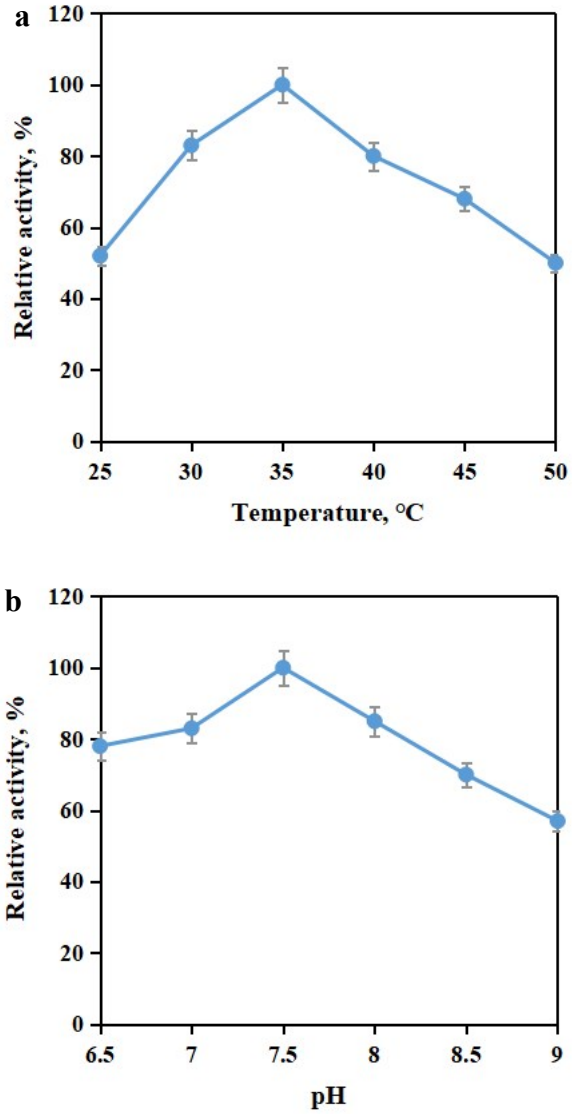

Fig. S6. Effects of various temperature on FF-amination activity of AT2018 cells (a); Effects of various pH on FF-amination activity of AT2018 cells (b).

Table S1. Changes of Sn content on Sn-graphite by element analysis before and after repeated use of Sn-graphite

Samples	Sn content, %
Fresh graphite	-
Sn-graphite	8.1
One-time recycled Sn-graphite	7.7
Five-time recycled Sn-graphite	2.9